The Effect of Capillary Number on a Condensate Blockage in Gas Condensate Reservoirs

Saifon DAUNGKAEW[1] and Alain C Gringarten[2]

School of Engineering and Resources[1], Walailak University, Thasala, Nakhon Si Thammarat 80160, Thailand.
Centre of Petroleum Studies[2], Department of Earth Resources and Engineering, Royal School of Mines Building, Prince Consort Road, London SW7 2 BP, UK.

ABSTRACT

In the petroleum industry, gas condensate reservoirs are becoming more common as exploration targets. However, there is a lack of knowledge of the reservoir behaviour mainly due to its complexity in the near wellbore region, where two phases, i.e. reservoir gas and condensate coexist when the wellbore pressure drops below the dew point pressure. The condensation process causes a reduction of the gas productivity (1). It has been reported in the literature that there is an increasing gas mobility zone due to a capillary number effect in the immediate vicinity of the wellbore in gas condensate reservoirs (2). This zone, called "velocity-stripping zone", compensates the well productivity loss due to the condensate drop-out. However, existence of this zone has just been recently found in an actual well test data (3,4). There is no conclusive study of this velocity-stripping zone in this type of reservoir. The objective of this study was to gain a better understanding of near wellbore effects in gas condensate reservoirs under production and well testing.

Key words: Gas condensate reservoirs - Condensate drop-out - Well test analysis - Velocity-stripping - A three-radial mobility zones - Well productivity

INTRODUCTION

Condensate reservoirs were not discovered until the early thirties. This is because gas condensate reservoirs are usually formed at higher pressure and temperature and are therefore typically deeper underground than other types of oil and gas reservoirs (5). Most known condensate reservoirs are found in the range of 3000 to 8000 psia and 200 to 400 ^{o}F (6). These gas condensate reservoirs have a wide range of fluid compositions. **Figure 1** exhibits a constant composition phase diagram of condensate reservoirs. As soon as the reservoir fluid has been produced, the bottomhole pressure starts to drop, and the first liquid occurs at the dew point pressure. As the flowing bottomhole pressure continues to drop at constant temperature (the phase diagram follows the constant temperature line 1-2-3), the condensate fraction increases until reaching a maximum. This process is known as retrograde condensation. Then the condensate fraction decreases as the pressure continues to drop due to revaporisation.

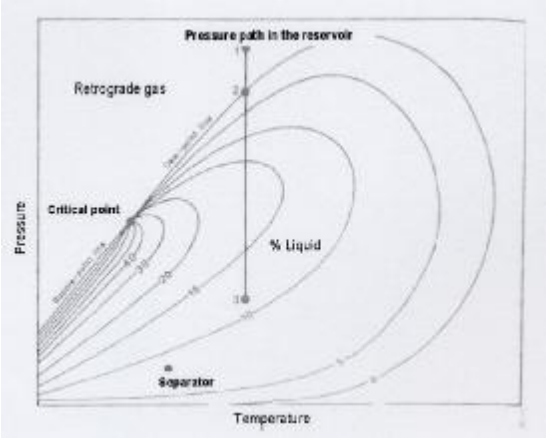

Figure 1. Constant composition diagram of a gas condensate system (7)

Muskat (5) first addressed the condensate blockage problem in gas cycling operations. After that many studies have shown a significant loss of well deliverability in gas condensate reservoirs due to condensate blockage (1,8,9). Well deliverability is affected by several natural parameters such as reservoir pressure, permeability, PVT properties, and time. It is also dominated by other production parameters, such as turbulence (non-Darcy flow, mechanical skin, and capillary pressure), multi-phase flow (relative permeability), and formation impairment (skin) (10).

Kniazeff and Naville (11) suggested that three radial zones appeared with different liquid saturations when the liquid condensate saturation reached a critical value. Away from the well, the reservoir fluid is the reservoir gas, therefore the liquid saturation within this zone equals the initial liquid saturation in the reservoir. In the second zone, liquid saturation varies with the gas effective permeability, and the fluid compositions also vary within this zone. The first zone corresponds to the near-wellbore. In this zone, the reservoir fluid presents as two phases, i.e. condensate liquid and reservoir gas. The composition of each phase is constant: the amount of condensate produced is equal to that flowing into the well. **Figure 2** shows the condensate saturation versus the radial distance in a three radial zone model. When the bottomhole pressure drops below the dew point pressure, the condensate bank starts to form in a reservoir. Only the gas phase could be produced at the surface before the condensate saturation reaches the critical value. Because of the lack of mobility of the condensate liquid phase, the composition of the system changes, the lighter components such as methane, ethane, and propane decrease, whereas the heaviest components (C7+) increase (5). When the liquid saturation reaches the critical condensate saturation, both gas and condensate start to flow to the well. At this stage, the phase diagram reaches the equilibrium saturation. Navosad (12) added that the changes in fluid composition resulted from changes in the fluid transported from the reservoir interior: first the rich (in place) gas, then the lean gas, and the revaporisation-enriched gas. It is evident that the details of composition evolution with time and distance are controlled by the production schedule, but the key point here is that a broad spectrum of fluid types exists at different points in time and space.

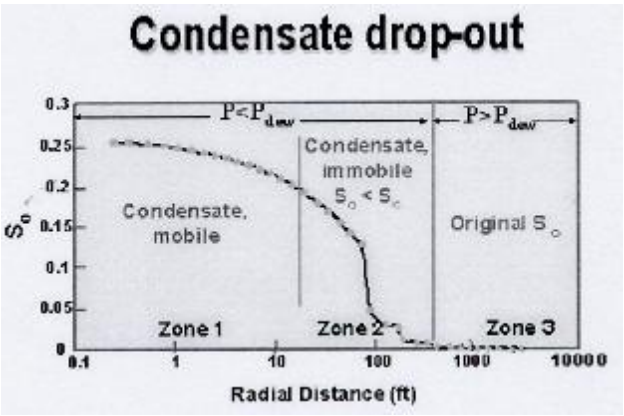

Figure 2. Condensate saturation profile of three-zone radial model (3)

It has been evident from the literature that in gas condensate reservoirs, there is an increasing mobility zone in the immediate vicinity of the wellbore (2). First indicated that the liquid saturation profile started from the original saturation at the external radius of the reservoir, and then increased until it passed though a maximum value before decreasing slightly near the wellbore. **Figure 3** shows a simulation where a condensate desaturation occurs near the wellbore. The increase in gas mobility is caused by greater gas and oil relative permeabilities with high flowrate and low IFT. The increased mobility zone causes a slight increase in well deliverability with time (2). Even in rich gas condensate reservoirs, well productivity initially decreases and then increases again as the reservoir is depleted (13). This is controlled primarily by the condensate saturation near the wellbore. As both liquid and gas around the wellbore change in composition, the liquid becomes heavier and the gas becomes leaner. As a result, the viscosity of the liquid becomes higher, and viscosity of the gas becomes lower with production. This improves the mobility of gas with respect to oil.

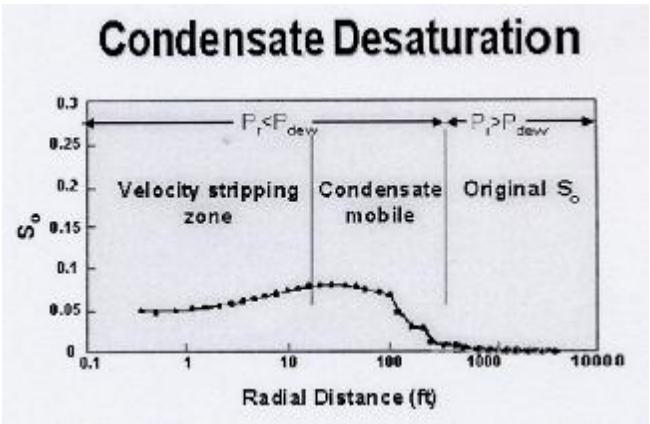

Figure 3. Condensate saturation profile with a desaturation condensate (3)

The increase in gas mobility zone or velocity-stripping zone has been found recently in the actual well test data (3,4). **Figure 4** indicates the physical behaviour in gas condensate reservoir as suggested in experimental studies (14). When the bottomhole pressure drops below the dew point pressure and the reservoir pressure is still above the dew point, the reservoir is divided into four radial zones. In terms of pressure derivative, the second zone and third would not show different mobilities. This is due to two reasons: (1) both zones will have high condensate saturation, and (2) the size of the second zone diminishes when the third zone is formed. When the velocity-stripping zone does not exist, there are only the two mobility zones as shown in **Figure 5.** The outer mobility zone indicates a gas reservoir with initial condensate saturation whereas the inner zone represents a mobility zone with high condensate saturation. In the near wellbore region (the third zone), where high velocity and low interfacial tension exist, the increased gas mobility zone occurs which is called the velocity-stripping zone. A three-mobility zone radial composite model can be used to represent this behaviour which yields three stabilisations on the derivative, as shown in **Figure 6.** The third stabilisation represents gas with lower condensate saturation.

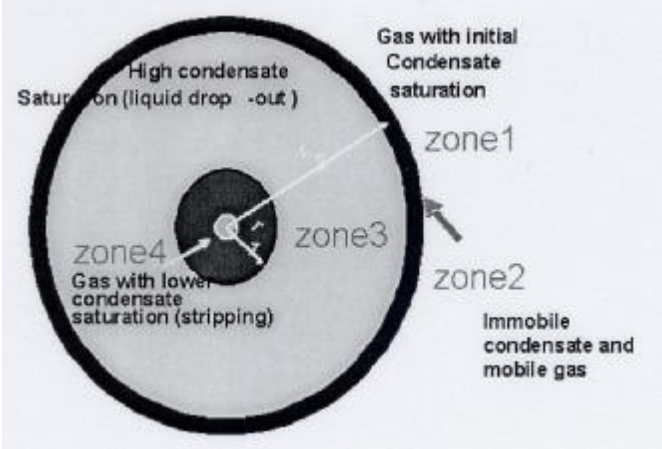

Figure 4. The four-radial composite model in a gas condensate reservoirs (3)

Well Test Analysis

- **Methodology**

First, a comprehensive and systematic interpretation procedure was used to analyse eight Drill Stem Tests (DST's) and three production well tests from an actual gas condensate field. A single-phase pseudo pressure introduced by Al-Hussainy et al (15) was used to plot pressure changes, and pressure derivatives because by this method different mobility zones, i.e. velocity-stripping, condensate bank, and the reservoir gas could be identified. Wellbore dynamics or phase redistribution is the main problem in the well test analysis of gas condensate reservoirs. This effect occurs when different phases flow in different directions in the wellbore (3). It increases wellbore storage in

both drawdown and build-up periods. It may dominate the test for many hours, and can be mistaken for a reservoir or condensate bank effect. Distinguishing wellbore phase redistribution effect from condensate bank effect is important in the analysis of gas condensate reservoirs. In this study, a normalised pressure and pressure derivative was used to plot different drawdown and build-up together (16). This method helps to compare pressure and pressure derivative of different flowrates in the same graph so that a final stabilisation representing the reservoir gas zone can be identified correctly using this plot.

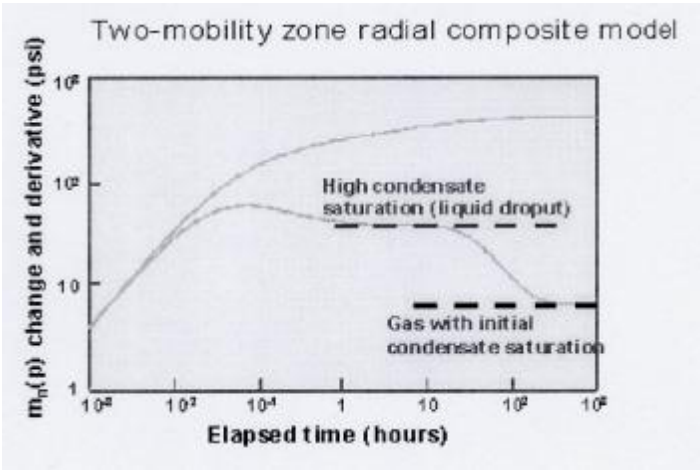

Figure 5. Two-mobility zone radial composite models generated by using analytical solution (3)

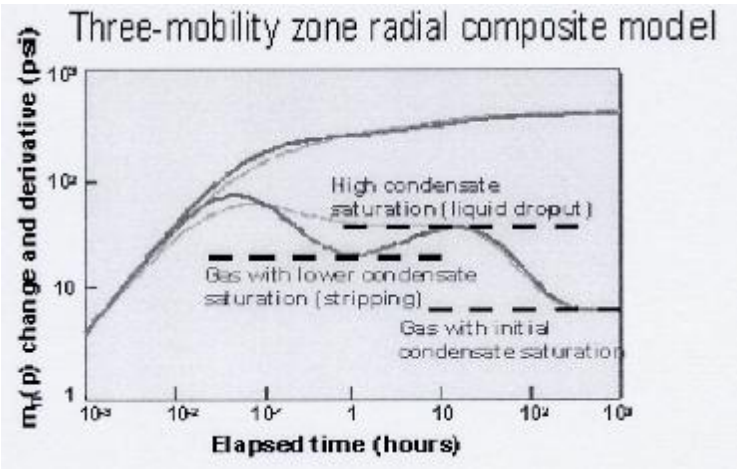

Figure 6. Three-mobility zone radial composite models generated by using analytical solution (3)

The velocity-stripping zone was then identified from the actual well tests. The near-wellbore, reservoir, and boundary behaviours were selected from the diagnostic plots of build-up and drawdown periods. Other tools such as analytical and numerical simulators can be used to distinguish between reservoir fluid effects and multi-layered or boundary effects.

- **Well Test Analysis Results in Actual Gas Condensate Reservoirs**

The velocity-stripping zone was identified in three drill stem tests (DST's) and one production well test, an example of which is shown in **Figure 7.** A three-mobility zone radial composite model presented by Satman (17) was then used to analyse these well tests. The radius of the velocity-stripping zone (r_1) was in the range of fifty to one hundred fifty feet, whereas the condensate bank radius (r_2) varied from fifty to one thousand two hundred feet. In five DST's and one production well test, only the decreased gas mobility zone due to condensate bank could be noticed, as shown in **Figure 8.** Thus, a two-mobility zone radial condensate reservoir was used to analyse these tests.

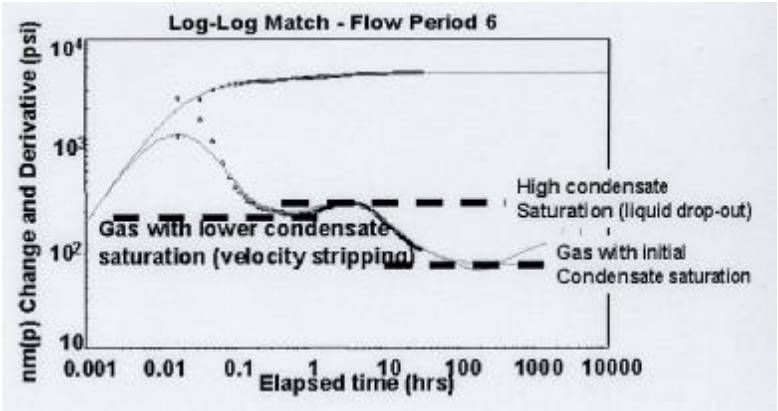

Figure 7. Example of the actual well test data in which the velocity-stripping zone can be identified in pressure derivatives

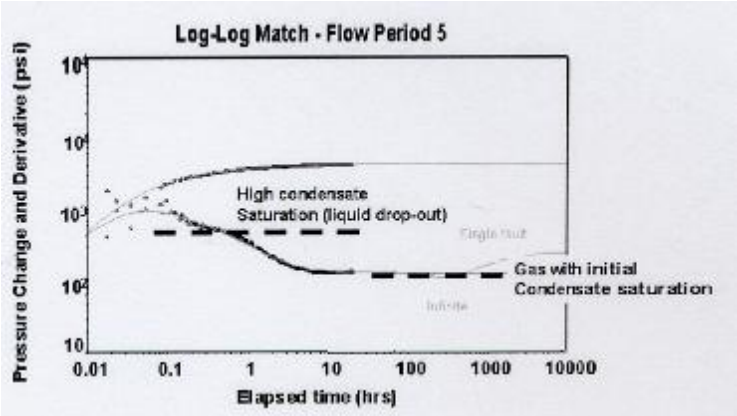

Figure 8. Example of the actual well test data in which only the condensate bank can be seen in pressure derivatives

Numerical Simulation

- **Methodology**

A single well model with 40 grid blocks the size of which increases logarithmically was simulated with the compositional simulator TechSim from AEA technology. One-dimensional flow was assumed in the reservoir. Wellbore storage and skin factor were not included in this model since the main concern for this simulation study was the effect of the condensate bank on pressure derivatives. The model with and without capillary number effects was simulated with a sequence of drawdown and build-up periods, as shown in **Figure 9 (a)**. The basic reservoir rock and fluid properties are given in **Table 1.** Two fluids were used in the simulation. Fluid A was a lean fluid which had a maximum liquid drop-out in constant volume depletion (CVD) of 1.5%. Fluid C was a rich fluid with a maximum liquid drop out of 15%. The compositions of fluids A and C are shown in **Table 2.** The lean gas condensate (fluid A) was modeled using the Soave-Redlich-Kwong (SRK) equation of state with 12 components including water while the rich gas condensate (fluid C) was modeled using the same equation of state with only 10 components

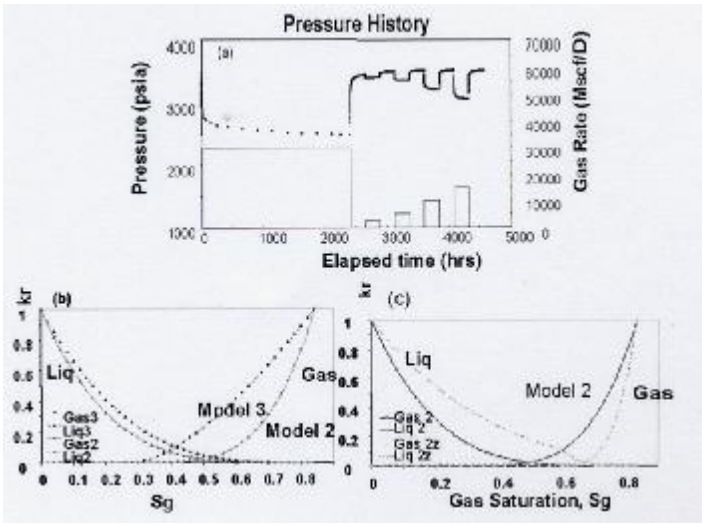

Figure 9. An example of pressure-rate history and relative permeability curves

Table 1. Basic reservoir rock and fluid properties for the simulation run

Characteristic	Value	
Porosity	0.1	
Absolute permeability	10 mD **	
Net to Gross ratio	1	
Connate water saturation	0.15	
Wellbore radius	0.25	Ft
Top depth	8500	Ft
Initial reservoir pressure (fluid A)	3600 **	Psia
Initial reservoir pressure (fluid C)	6400 **	Psia

The star sign (**) in Table 1 indicates the parameters that are changed in some simulation runs so as to see the effects of initial reservoir pressure.

The effects of interfacial tension were included into the compositional simulator Techsim by implementing the method proposed by Coats (18). Coats suggested that the gas/oil interfacial tension could be calculated from the Macleod-Sugden correlation.

$$s^{1/4} = \sum_{i=1}^{n} P_{chi}\left(r_L x_i - r_g y_i\right) \qquad \textbf{Equation 1}$$

where P_{chi} is the parachor of component i and density is in the units of g-mol/cm^3. x_i and y_i are the liquid and gas mole fraction of component i, respectively. The liquid and vapour phase molar density is converted to g-mol/cm^3. In order to calculate the interfacial tension using **Equation 1**, the flash calculation using the pressure from each

gridblock was performed when the gas and liquid molar density, and the composition of each component were obtained using the PVT software PVTSim (CalSep A/S).

Table 2. Fluid composition of fluids A and C. (Al-Lamki , 1999).

Fluid A		Fluid C	
Component	**Mole Fraction**	**Component**	**Mole Fraction**
N2	0.0158	-	-
CO2	0.0241	CO2	0.0353
C1	0.796	C1+N2	0.6596
C2	0.0687	C2	0.1008
C3	0.0357	C3	0.0462
n-C4	0.0189	n-C4	0.0267
n-C5	0.0088	n-C5	0.0334
PC1	0.0262	PC1	0.0709
PC2	0.0046	PC2	0.02241
PC3	0.0012	PC3	0.00469
PC4	0	-	-
pseudo components			
PC1	C6 to C10	PC1	C6 to C10
PC2	C11 to C15	PC2	C11 to C20
PC3	C16 to C29	PC3	C20+
PC4	C30+		

Capillary number (N_c) is a function of fluid viscosity (μ), velocity (v) and the interfacial tension (σ) as shown in the following equation:

$$N_c = \frac{v\mu}{\sigma} \qquad \textbf{Equation 2}$$

If the fluid viscosity is assumed not to change much with pressure, the capillary pressure is only a function of fluid velocity and interfacial tension. In addition, fluid velocity increases towards the wellbore in inverse proportion to the radial distance.

$$v = \frac{Q}{2\pi rh} \qquad \textbf{Equation 3}$$

where Q is the flowrate, r is the wellbore radius, and h is the reservoir thickness.

- **Simulation Results and Discussion**

The first model was run with capillary number effect using lean fluid A, relative permeability no. 2, and the initial pressure was much higher than the dew point pressure, as shown in **Figure 10.** As to be expected, there was no condensate drop-out in the near wellbore region since the flowing bottomhole pressure was much higher than the dew point pressure. The log-log plot of all build-up and drawdown periods is shown in **Figure 11**. The gas effective permeability stabilised at the input value (10 mD). This result confirmed that the simulator calculates the correct pressure transient data. In addition, the liquid saturation was found to be zero at the end of all drawdown periods. The liquid saturation was zero for all gridcells since the bottomhole flowing pressure (BHFP) was higher than the dew point pressure. The vapour and water saturations were constant for the entire radial distance. The capillary number was found to be zero in all gridblocks because only gas was present. In other words, the interfacial tension for each gridblock could not be calculated since there was only a single phase in a system. Next, the simulation was run with lower initial reservoir pressure **(Figure12)**. From this figure, the first drawdown and second build-up period was higher than the dew point pressure. The drawdown period pressure in the third period droped below the dew point pressure at about 500 hours. Pressure derivative of the first drawdown and second build-up was located at the gas effective permeability (10 mD) similar to **Figure 11.** As soon as the BHFP droped lower than the dew point pressure, the condensate started to form in the reservoir. **Figure 13** shows pressure as a function of radial distance in a semilog scale. At the of about 20 ft from the wellbore, pressure droped below the dew point pressure and the liquid phase occured in the system. As a result, the vapour phase saturation decreased and the liquid phase increased near the wellbore. **Figure 14** shows that the capillary number is at the maximum point in the near wellbore region. This figure also shows that the velocity is at the maximum at the near wellbore region **(Equation 2)**. The interfacial tension was found to increase at the distance near the wellbore **(Figure 15)**. **Figure 16** shows the plot between the interfacial tension and gridblock pressure. The interfacial tension increased as the gridblock pressure decreased. This is because more condensate drop-out at the near wellbore region results in a greater difference in liquid and vapour terms, as shown in **Equation 1**. As a result, a higher interfacial tension was seen in the near wellbore region. The capillary number was found to increase with decreasing gridblock pressure, as also shown in this figure.

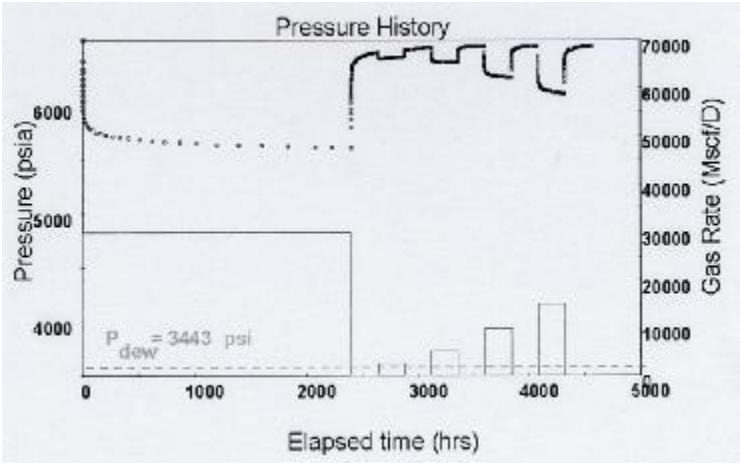

Figure 10. Pressure and flowrate profiles of lean fluid A when the flowing bottomhole pressure is much higher than the dew point pressure

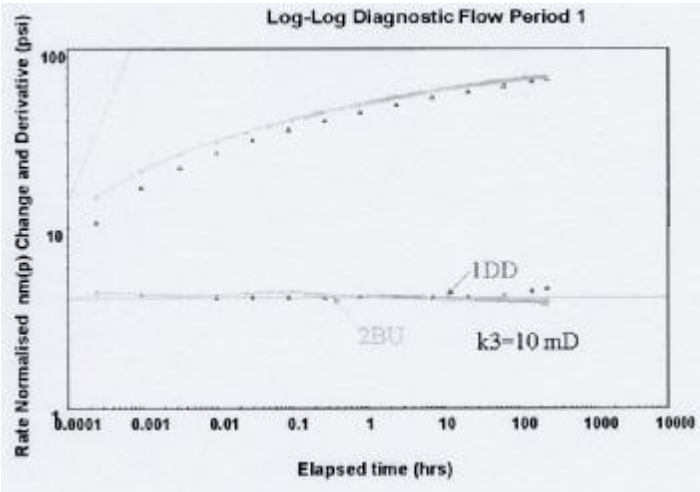

Figure 11. A log-log plot of all periods when the flowing pressure is higher than the dew point pressure

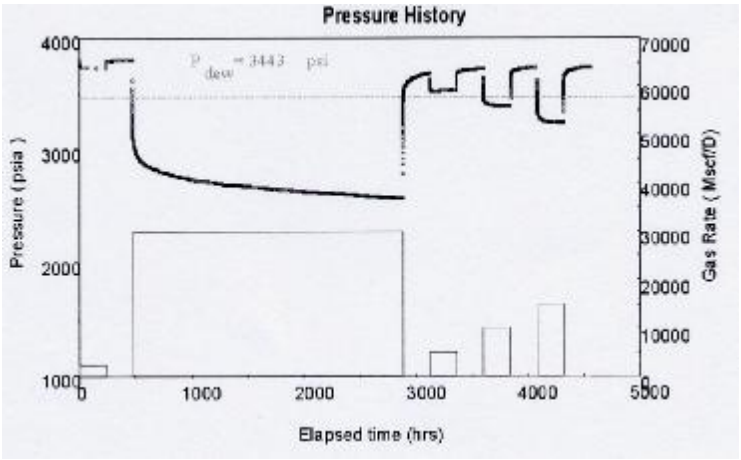

Figure 12. Pressure and flowrate profiles using lean fluid A, relative permeability curves no. 2 and initial reservoir pressure is 3800 psia

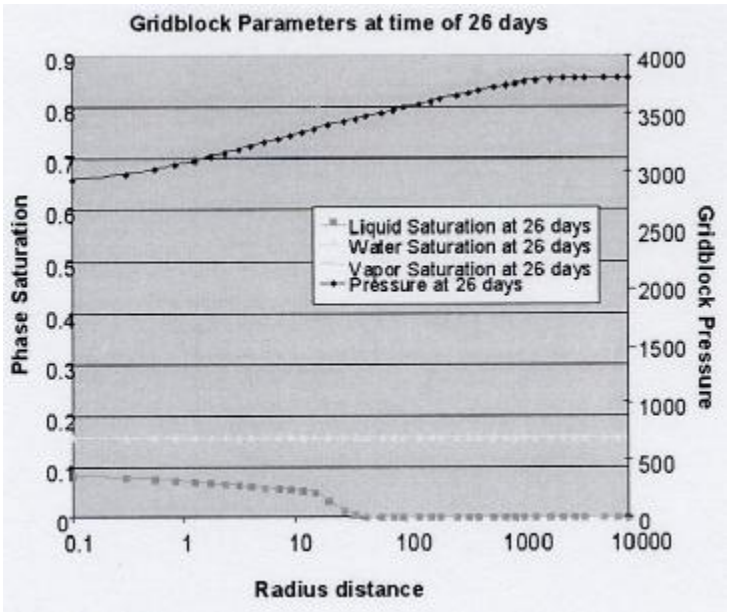

Figure 13. Gridblock parameters as a function of radial distance

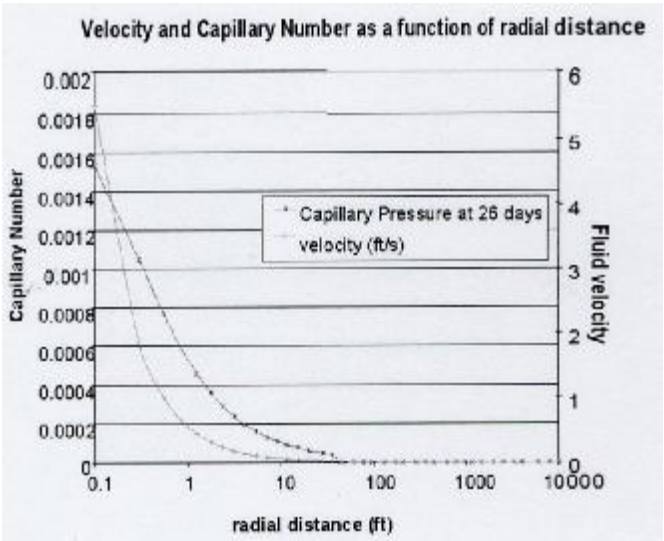

Figure 14. Velocity as a function of radial distance

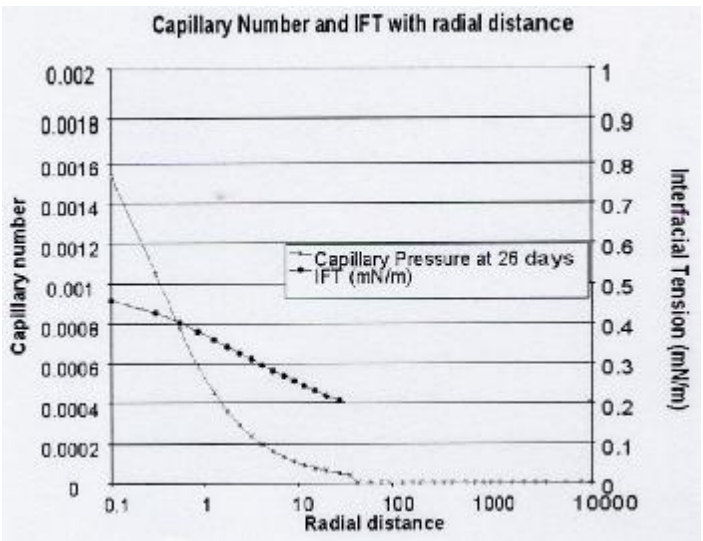

Figure 15. Interfacial tension as a function of radial distance

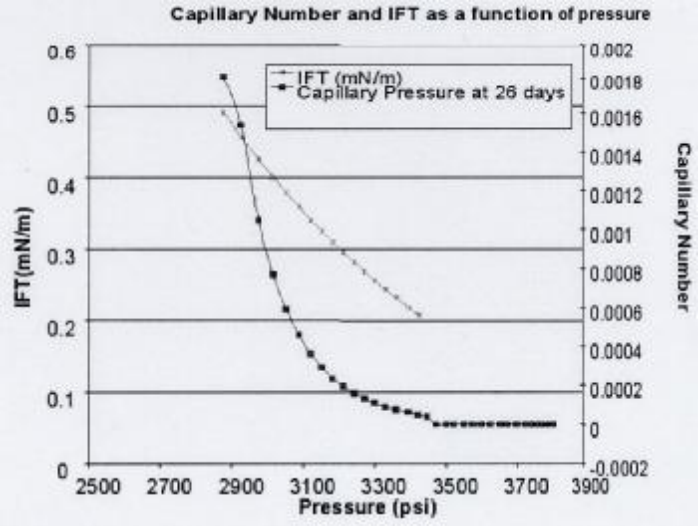

Figure 16. Interfacial tension as a function of pressure

- **Effect of Capillary Number (N_C)**

Two simulations were run for fluid A with the initial reservoir pressure of 3600 psia, and the BHFP dropped below the dew point pressure as soon as the well started to produce. The flowrate of DD1, DD3, DD5, DD7, and DD9 are 30, 2.5, 5, 10, and 15 MMSCFD respectively. The capillary effect was the control parameter in these two runs. The results generated from the model without and with the capillary number effect are shown in **Figure 17** and **Figure 18** respectively. Since the BHFP droped below the dew point pressure as soon as the well started to produce, a condensate bank was formed straight away, as can be seen at 0.1 day **(Figure 17)**. The condensate saturations at time 0.1, 1, 10 and 100 days of the 1DD are plotted in these two figures. The condensate saturation was found to increase with the production time. A model without the capillary number effect indicated higher condensate saturation than that of one with the Nc effect. The saturation profile without the capillary number effect was characterised by a bell shape **(Figure 17)** where the highest condensate saturation was located at the region nearest to the wellbore. In contrast, the saturation profile of a model with the Nc effect was found to increase in a direction approaching the wellbore, decreasing again in the near wellbore region **(Figure 18)**. The saturation profile of a model with capillary number effect can be best characterised by a donut shape. As shown in **Figure 18**, a diagnostic log-log plot of three-radial composite reservoir on the right-hand side (3) indicates a similarity in the shape of the condensate saturation (as shown in the left hand side). A three-mobility zone radial composite model can be identified in both figures. The outer zone represents the gas with the initial condensate saturation. The second zone indicates a zone with high condensate

saturation. The near wellbore shows the zone with increasing gas mobility or 'velocity-stripping zone'.

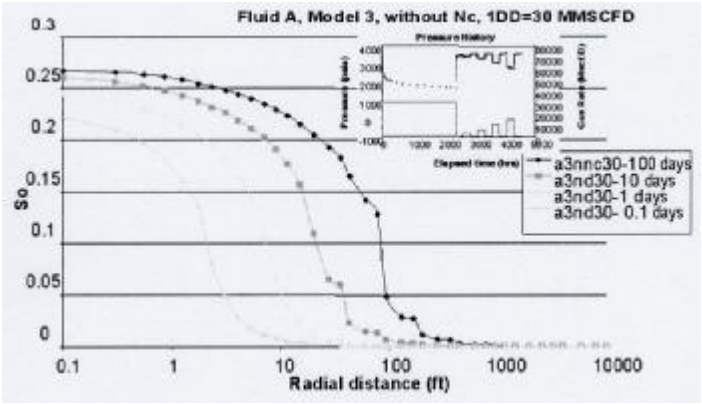

Figure 17. Effect of the duration of the first drawdown period (lean fluid, without Nc)

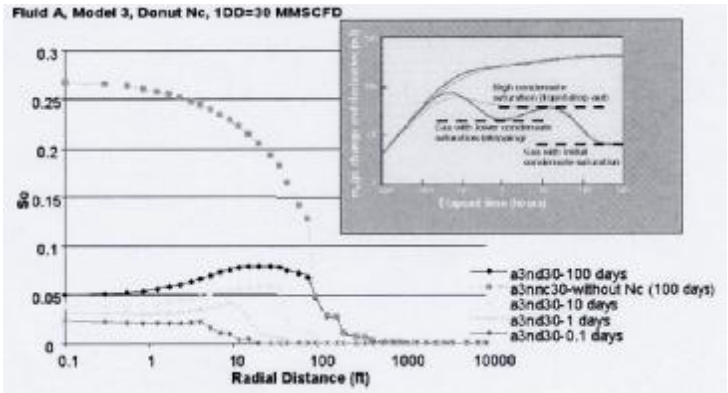

Figure 18. Effect of the duration of the first drawdown period (lean fluid, with Nc)

As expected, the model without capillary number yielded more reduction in reservoir pressure, and a greater reduction in the gas relative permeability. Consequently, it can be concluded that with velocity-stripping effect, a smaller condensate bank forms in the reservoir, as can be seen in the log-log plots in **Figure 19** and **Figure 20**, respectively. The derivative from the simulation with the capillary number effect also displayed the three stabilisations **(Figure 20)**.

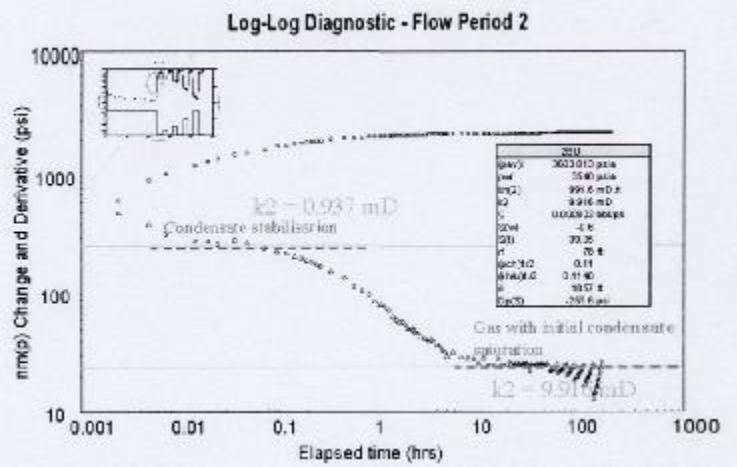

Figure 19. Log-log diagnostic plot of 2BU of a rich fluid without Nc effects

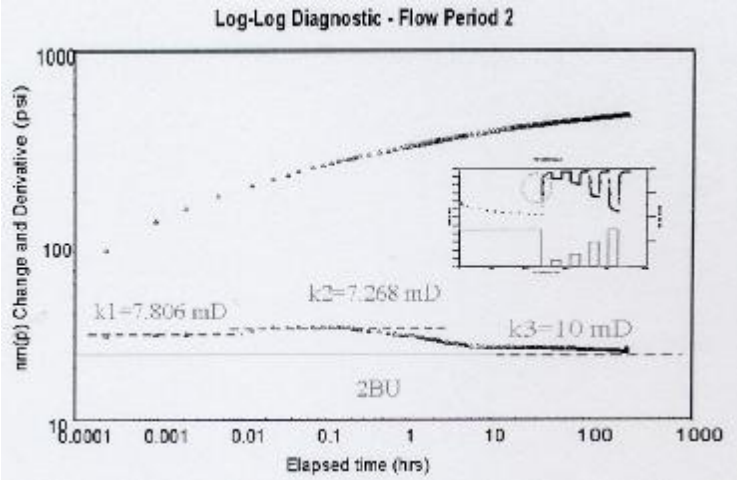

Figure 20. Log-log diagnostic plot of 1DD of a lean fluid with Nc effects

- **Effect of Reservoir Fluids**

Figure 21 and **Figure 22** indicate saturation profiles of the simulation using rich gas condensate fluid with and without capillary number effect. Similar to the lean fluid A, the model with Nc effect resulted in a lower condensate saturation near the wellbore compared to that from a model without capillary number effect. The log-log

plots of these two runs are shown in **Figure 23** and **Figure 24**. Both log-log and saturation profile plots for the rich fluid indicate different shapes from the plot of the lean fluid. For the rich fluid, even though the capillary number was included in the model, the increased gas mobility zone could not be seen in either the log-log or saturation profile plots.

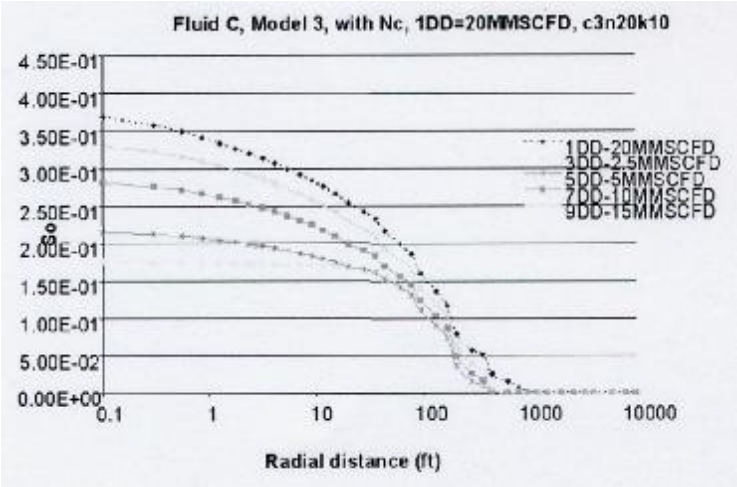

Figure 21. The Nc effect on saturation profile of Rich Fluid, with Nc effect

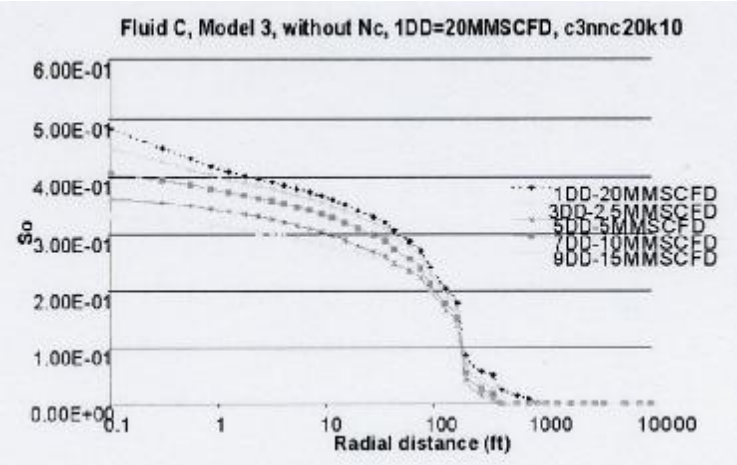

Figure 22. The Nc effect on saturation profile of Rich Fluid, without Nc effect

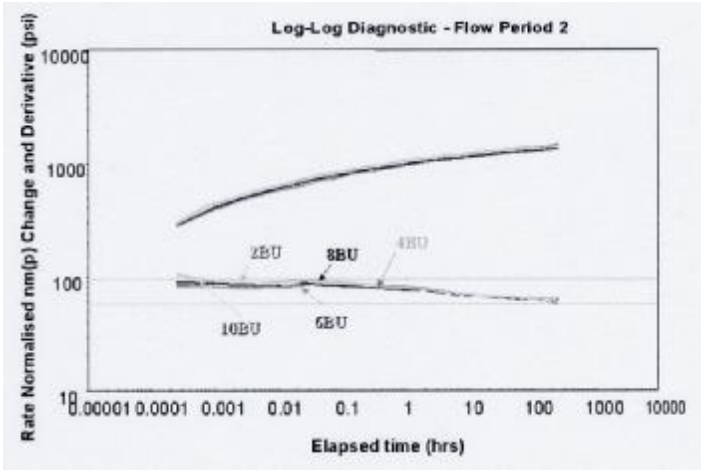

Figure 23. The Nc effect on log-log plot of Rich Fluid, with Nc effect

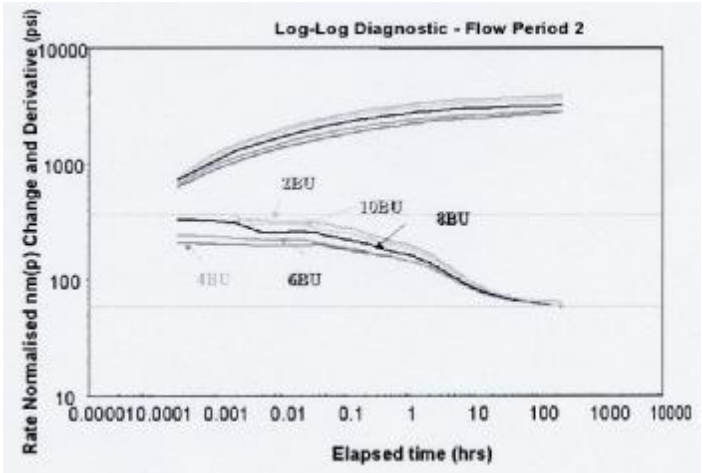

Figure 24. The Nc effect on log-log plot of Rich Fluid, without Nc effect

In order to explain why the velocity-stripping zone can be seen in the lean gas condensate fluid, but not in the rich one, the saturation and relative permeability curves were plotted on the same graphs in **Figure 25** and **Figure 26** for fluid A and C respectively. For the lean fluid, the condensate saturation increased towards the wellbore until it reached the maximum point and then decreased again near the wellbore. The gas relative permeability decreased to a minimum value before increasing again. The maximum and minimum points of the condensate saturation and

the gas relative permeability could not be noticed in the rich fluid. The saturation profile of these two fluids using the relative permeability curve no. 2 with capillary number effect and a 1DD of 30 MMSCFD is shown in **Figure 27**. It can be seen clearly that the rich fluid had greater condensate saturation than the lean fluid. In addition, the shapes of saturation profiles were different. **Figure 28** shows the capillary number as a function of radial distance of fluid A and fluid C at the time of 100 days. It is clear in this figure that even though capillary number effect in the rich fluid was higher than that in the lean fluid, the capillary number effect could not compensate for the effect of fluid richness in the system. As a result, rich fluid C had higher condensate saturation than the lean fluid **(Figure 27)**.

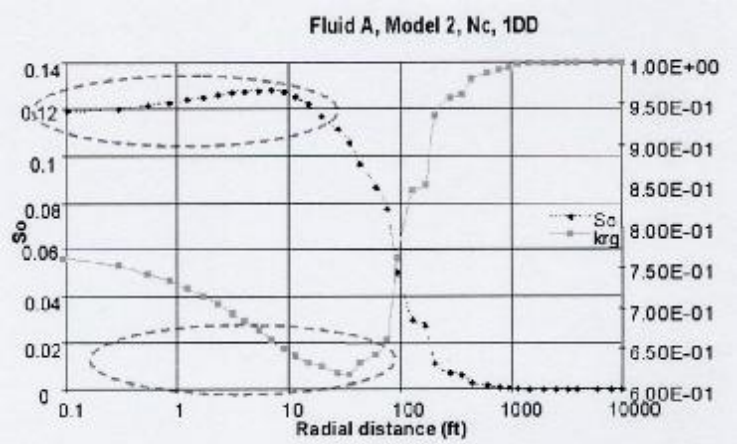

Figure 25. Saturation profile and gas relative permeability curves of lean fluid A

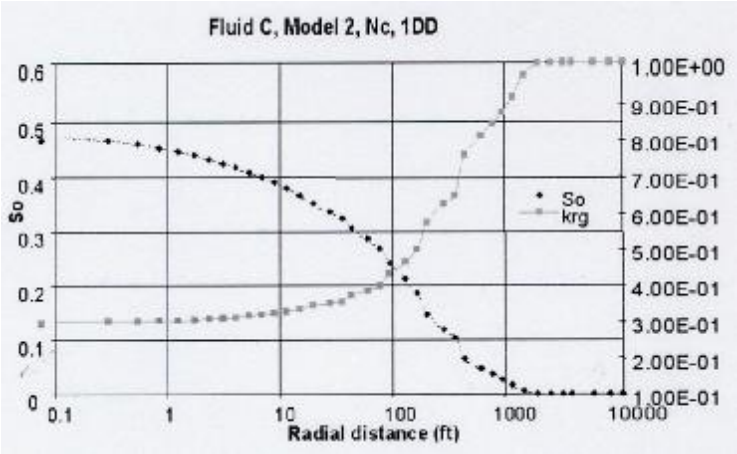

Figure 26. Saturation profile and gas relative permeability curves of rich fluid C

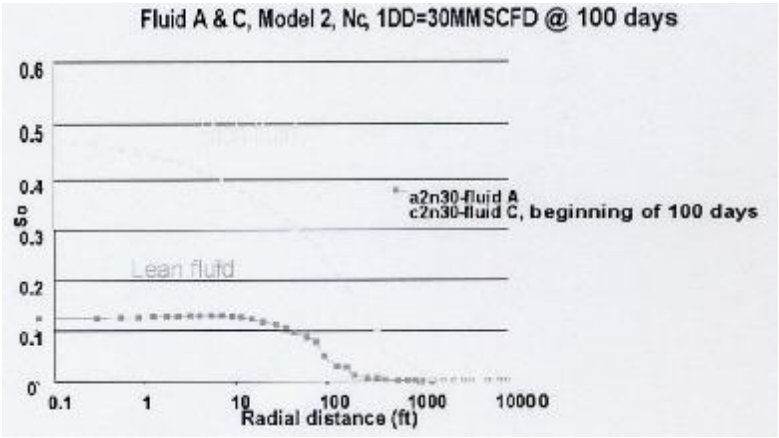

Figure 27. Saturation profile between two fluids with Nc

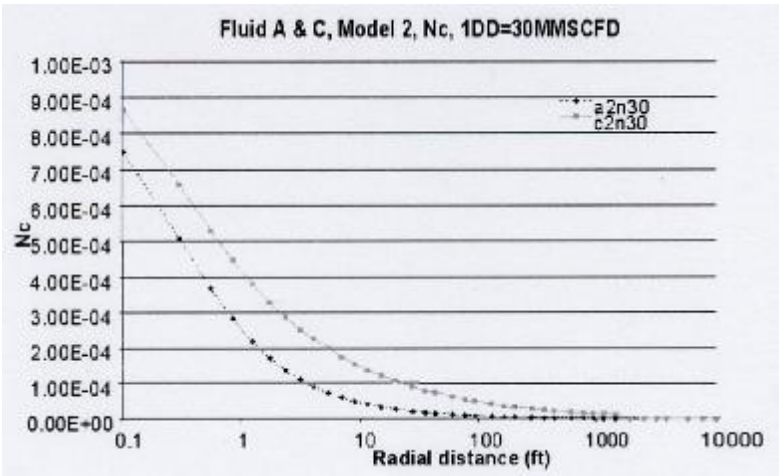

Figure 28. Capillary number of two fluids with Nc

- **Simulation Results for the Actual Field Data**

A single well compositional simulation model was constructed using the actual reservoir fluid which was provided from a fluid sampling from the actual well testing. The reservoir fluid of this selected field was characterised as relatively lean gas condensate since the maximum liquid drop-out in two production areas was not large, between 8% and 5.6%. The input parameters are shown in **Figure 29.** The simulation results are then compared with the actual well test data. Five DST were selected from twelve actual well tests according to the existence of a condensate bank and data availability, i.e. wells 1 to 5. Two production well tests were also simulated, i.e. wells 6 to 7.

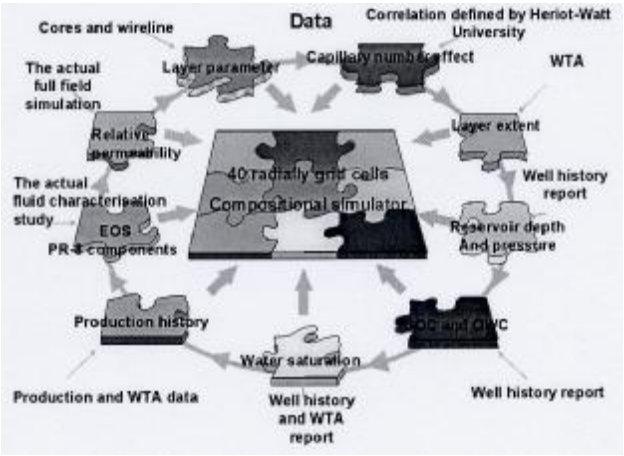

Figure 29. Input parameter for a single well simulation

In all these seven well tests, the simulation model with capillary number effect could match the actual test better than the model without capillary number effect. The latter model caused too high a pressure drop in the reservoir, which made it impossible to match the actual tests. This finding confirmd that the velocity-stripping effect exists in both production areas in this selected gas condensate field. In all simulated pressure transient tests, the velocity-stripping zone could be seen in the condensate saturation curve plotted versus the radial distance. However, only three sets of simulated data, which include one production well test (well 6), and two DST tests (wells 2, and 3) showed the presence of an increased gas mobility zone in the derivative plot. Another production and three DST pressure transient tests were found not to show a zone with increasing gas mobility in the log-log plot. In these wells, the condensate saturation was not significant enough and the velocity-stripping zone could not be observed in pressure derivatives. It was concluded that the oil saturation needs to be equal or higher than 20% in order to see the increased mobility zone in the pressure derivative data. **Table 3** shows the condensate saturations from the simulation of seven pressure transient tests.

Table 3. The simulation result for the actual gas condensate field

Wells	So	So	Condensate Bank radius	
	Condensate Bank	Velocity-Stripping	WTA	Simulation
4	0.09	0.07	86	10
7	0.1	0.06	0	1
1	0.2	0.15	42-65	29
2	0.35	0.31	112	5
3	0.55	0.5	52	50
5	0.10-0.15	0.2	-	30
6	0.27	0.15	1113	100

A comparison between the actual and simulated pressure transient tests indicated that the velocity-stripping zone should exist in all well tests in a particular field. However, in practice, this zone could not be seen in most pressure transient responses. The reasons for the non-appearance of this zone in the actual pressure transient test were: (1) The maximum condensate saturation near the wellbore was not significant enough; (2) Wellbore storage effects at early times hided the increased gas mobility zone; (3) The duration of the test was not long enough; (4) The quality of pressure data was not good enough; and (5) Phase redistribution effects occured the wellbore.

Table 3 indicates that the condensate bank radii from the simulations of most wells were underestimated compared to the actual well tests, especially in production well 6. However, the simulated pressure transient tests in well 5 match the pressure transient from the actual well test (as shown in **Figures 30 and 31**). The pink line in these two figures indicates the simulation results whereas the blue dots represent the actual pressure response data. Well 5 was simulated using its PVT sample. The EOS in the simulation of well 5 provided a good match in terms of the produced gas and oil rates. In the actual well test, the condensate bank could not be seen due to high wellbore storage, but the simulation indicates a 80 ft radius condensate bank.

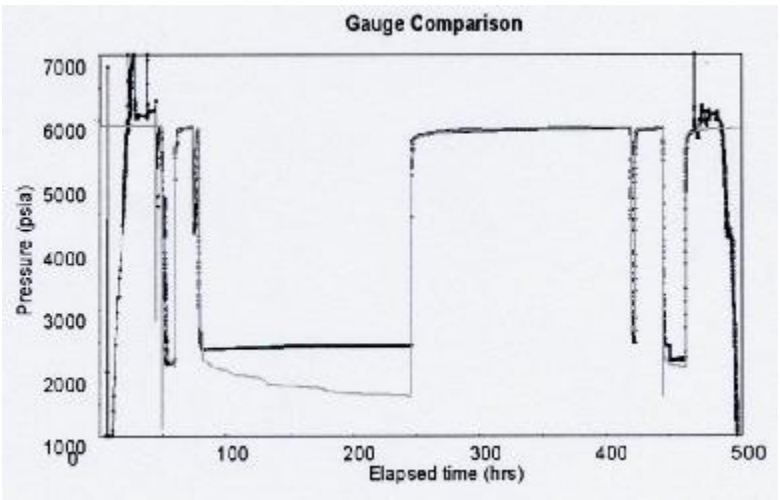

Figure 30. A comparison between the actual and the simulated pressure transient tests

In addition, the PVT samples for the other wells were found not to be valid when the quality checks were performed. This means that the sampling fluid did not represent the actual reservoir fluid. It might be due to some operation problems when the fluid sampling was taken from the reservoir or an error in the laboratory experiment process. As a result, their PVT data could not be used in the simulation. When the fluid from well 5, which was leaner that other wells, was used to simulate condensate bank in other wells, the simulated fluid was underestimated. This suggested that PVT properties were the main issue in the simulation of gas condensate reservoirs. The fluid properties of each well are different even though all wells had the same

originated reservoir fluid. This is due to production profile. i.e. production rate, local reservoir pressure, etc. These parameters caused the changes in fluid properties in each well. As a result, the validated local PVT sampling is required in order to obtain a matching for the condensate bank radius.

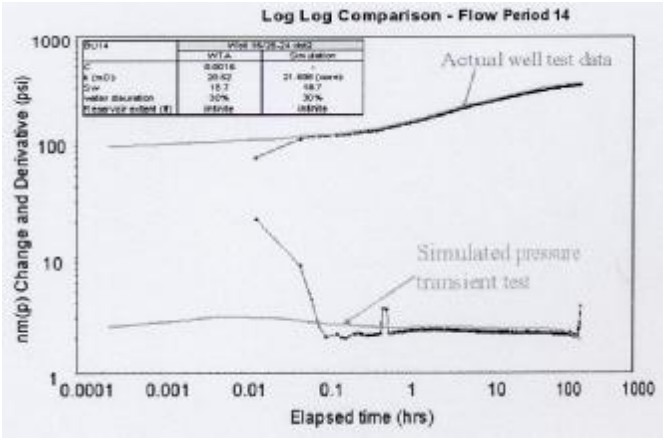

Figure 31. A log-log match between the actual and simulated pressure of DD14

CONCLUSION

The velocity-stripping zone could be identified from the actual well test data. The results from numerical simulation also showed the existence of this increased mobility zone. However, this zone could not be identified in all well test data due to several reasons: (1) The maximum condensate saturation near the wellbore was not significant enough; (2) Wellbore storage effects at early times hided the increased gas mobility zone; (3) The duration of the test was not long enough; (4) The quality of pressure data was not good enough; and (5) Phase redistribution effects occured in the wellbore. The PVT properties were found to be the most important parameter in the simulation of gas condensate reservoirs.

ACKNOWLEDGEMENTS

I would like to thank Professor Alain C Gringarten for his outstanding contribution and guidance. I am particularly grateful to him, Britannia Operator Ltd, and the Royal Thai Government for their financial support. I also would like to thank the following people for their discussion: Tim Whittle, Ali Al-Lamki, Prof Blunt, Florian Hollaender, Thomas von Schroeter, Djamel Ouzzane, Fraser Ross, and Andy Scott.

REFERENCES

1) Fussell DD. Single-well performance predictions for gas condensate reservoirs. *J Petroleum Tech 1973; 860-70.*
2) Gondouin M Iffly R Husson J. An attempt to predict the time dependence of well deliverability in gas-condensate fields. *Soc Petroleum Engineer J 1967; 112-24.*
3) Gringarten AC Al-Lamki A Daungkaew S Mott R Whittle T. Well test analysis in gas-condensate reservoirs, SPE62920, paper presented at the SPE Annual Technical Conference and Exhibition held in Dallas, Texas, October 1-4, 2000.
4) Daungkaew S Gringarten AC. Well test investigation of condensate drop-out behaviour in a North Sea lean gas condensate reservoir, SPE77548, paper presented at the 2002 SPE Annual Technical Conference and Exhibition held in San Antonio, Texas, 29 September – 2 October , 2002.
5) Muskat M. Physical Principle of Oil Production, McGraw-Hill Book Co, Inc, New York, 1949, p. 793.
6) Bradley HB. Petroleum Engineering Handbook, Society of Petroleum Engineers, USA, 1992.
7) McCain WD Jr. The Properties of Petroleum Fluids, Penn Well Publishing Company, USA, 1990.
8) Favang¸Whitson CH. Modelling gas condensate well deliverability, SPE30714, paper presented at the SPE Annual Technical Conference and Exhibition, Dallas, Texas, October 22-25, 1995.
9) Barnum RS Brinkman FP Richardson TW Spillette AG. Gas condensate reservoir behaviour: productivity and recovery reduction due to condensation, SPE30767, paper presented at the SPE Annual Technical Conference and Exhibition, Dallas, Texas, October 22-25, 1995.
10) Al-Shaidi SM. Modelling of Gas-Condensate Flow in Reservoir at Near Wellbore Conditions, Thesis Submitted for the Degree of Doctor of Philosophy in Petroleum Engineering, Department of Petroleum Engineering, Heriot-Watt University, UK, August, 1997.
11) Kniazeff VJ Naville SA. Two-phase flow of volatile hydrocarbons. *Soc Petroleum Engineer J 1965; 37.*
12) Novosad Z. Compositional and phase changes in testing and producing retrograde gas wells, SPE35645, paper presented at the Gas Technology Conference, Calgary, Alberta, Canada, 28 April - 1 March, 1996.
13) El-Banbi AH McCain WD Jr Semmebeck ME. Investigation of well productivity in gas-condensate reservoirs, SPE59773, paper presented at the 2000 SPE/CERI Gas Technology Symposium held in Calgary, Alberta, Canada, April 3-5, 2000.
14) Ali JK McGauley PJ Wilson CJ. Experimental studies and modelling of gas condensate flow near the Wellbore, SPE39053, paper presented at the Fifth Latin American and Caribbean Petroleum Engineering Conference and Exhibition, Rio de Janeiro, Brazil, 30 August - 3 September, 1997.
15) Al-Hussainy R Ramey HJ Jr Crownford PB. The flow of real gases though porous media. *J Petroleum Tech 1996; 624-36.*
16) Raghavan R Chu W Jones J. Practical considerations in the analysis of gas condensate well test SPE30576, paper presented at the 70th Annual Technical Conference and Exhibition of the Society of Petroleum Engineers, Dallas, Texas, October 22-25, 1995.
17) Satman A Eggenschwiler M Ramey HJ Jr. Interpretation of injection well pressure transient data in thermal oil recovery SPE8908, paper presented at the 50th Annual California Regional Meeting of the Society of Petroleum Engineers of AIME, Log Angeles, California, April 9-11, 1980.

18) Coats KH. An equation of state compositional model SPE8284, paper presented at the 54th Annual Fall Technology Conference and Exhibition of the Society of Petroleum Engineers, Las Vegas, Nevada, US, September 23-26, 1979.

บทคัดย่อ

สายฝน ดวงแก้ว[1] และ Alain C Gringarten[2]

ผลของ capillary number ต่อการกลั่นตัวของของเหลวในแหล่งผลิตที่เป็น gas condensate

อุตสาหกรรมปิโตรเลียมในปัจจุบันได้มีการค้นพบและผลิตของไหลจากแหล่งกักเก็บที่มีของไหลประภท gas condensate มากยิ่งขึ้น แต่ปัญหาสำหรับการผลิต คือ คุณสมบัติของของไหล gas condensate จะมีความซับซ้อนกว่าของไหลชนิดอื่น เพราะของไหลชนิดนี้ประกอบด้วยของเหลว (condensate) และก๊าซธรรมชาติ ซึ่งพฤติกรรมการเปลี่ยนแปลงคุณสมบัติระหว่างของเหลวและก๊าซในแหล่งผลิตปิโตรเลียมชนิดนี้ยังไม่เป็นที่ทราบกันอย่างแน่ชัด ทำให้การวางแผนและควบคุมการผลิตเกิดความยุ่งยาก โดยปัญหาที่พบส่วนใหญ่ คือกำลังการผลิตของหลุมขุดเจาะ (well productivity) สำหรับของไหลชนิดนี้จะลดลงอย่างรวดเร็วเมื่อความดันที่หลุมขุดเจาะลดลงต่ำกว่าความดันอิ่มตัว (dew point pressure) เนื่องจากของเหลวจะกลั่นตัวออกมาจากก๊าซธรรมชาติ และจะทำให้ความสามารถในการไหลของก๊าซธรรมชาติลดลง

ในการวิจัยเรื่อง gas condensate reservoir ได้มีการค้นพบว่าค่า capillary number สามารถช่วยเพิ่มความสามารถในการเคลื่อนที่ (mobility) ของก๊าซรอบหลุมขุดเจาะ ซึ่งจะส่งผลทำให้กำลังการผลิตของหลุมขุดเจาะเพิ่มขึ้น และบริเวณรอบหลุมขุดเจาะที่มีการเพิ่มขึ้นของ gas mobility เรียกว่า velocity-stripping zone แต่ทั้งนี้การบ่งชี้ velocity-stripping จากข้อมูลที่ได้จากการทดสอบหลุมจริง (well testing) เพิ่งมีการค้นพบได้ไม่นานโดย Gringarten et al (3) และ Daungkaew et al (4) อีกทั้งยังไม่มีการศึกษาและสร้างแบบจำลองสำหรับ gas condensate reservoir โดยละเอียด ดังนั้น งานวิจัยนี้จึงมีวัตถุประสงค์เพื่อศึกษาผลของ velocity-stripping zone ใน gas condensate reservoir ทั้งในข้อมูลที่ได้จากการทดสอบหลุมจริง และในแบบจำลองทางคณิตศาสตร์ (numerical simulation)

[1] สำนักวิชาวิศวกรรมศาสตร์และทรัพยากร มหาวิทยาลัยวลัยลักษณ์ อำเภอท่าศาลา จังหวัดนครศรีธรรมราช 80160

[2] Centre of Petroleum Studies[2], Department of Earth Resources and Engineering Royal School of Mines Building, Prince Consort Road, London SW7 2 BP, UK